jove | Bioengineering

DATE PUBLISHED November 13, 2026
DOI 10.3791/74185
URL jove.com/t/74185

Biofilm Lithography for Controlled Measurements of Electroactive Bacteria on Electrodes

Fengjie Zhao[1], **Marko S. Chavez**[1,2], **Joshua T. Atkinson**[1,2,3], **James Q. Boedicker**[1,4], **Mohamed Y. El-Naggar**[1,4,5]

[1]Department of Physics and Astronomy, University of Southern California [2]Omenn-Darling Bioengineering Institute, Princeton University [3]Department of Civil and Environmental Engineering, Princeton University [4]Department of Biological Sciences, University of Southern California [5]Department of Chemistry, University of Southern California

✉ *Corresponding Author : Fengjie Zhao <fengjiez@usc.edu>*

Citation

Zhao, F., Chavez, M.S., Atkinson, J.T., Boedicker, J.Q., El-Naggar, M.Y. Biofilm Lithography for Controlled Measurements of Electroactive Bacteria on Electrodes. *J. Vis. Exp.* (237), e74185, doi:10.3791/74185. (2026).

Abstract

Electroactive microbes can form conductive biofilms that serve as living electronic biomaterials, integrating the dynamic functionality of living cells with the input-output properties of electronic components. Creating these living electronics requires precise control over biofilm formation on solid-state electrodes to characterize and harness the electronic properties of the biotic-abiotic hybrids. However, native biofilm formation on electrode surfaces often results in films that are non-uniform or too thin for reliable and reproducible electronic measurements and applications. Here, a protocol is presented that utilizes a light-induced genetic circuit in the model electroactive bacterium *Shewanella oneidensis* to enable the precise spatial patterning of conductive biofilms on electrodes using light. This so-called biofilm lithography approach can be performed using either a simple projector or a light-emitting diode array. The controlled patterning allows for tunable biofilm conduction dependent on pattern size. By utilizing these defined geometries and measuring the resulting conduction currents through biofilms, this method enables accurate quantification of the intrinsic living material conductivity. Overall, this protocol presents a facile approach for controlling electroactive biofilm formation on electrodes, which may facilitate further advances in both studying and harnessing bioelectronics.

Introduction

Electroactive microbes can respire external solid surfaces such as minerals and electrodes in anoxic environments through a process known as extracellular electron transfer (EET)[1,2,3]. EET has been widely studied in the model electroactive organisms *Shewanella oneidensis* and *Geobacter sulfurreducens*[1,2]. These bacteria utilize a network of cytochromes spanning the inner membrane, periplasm, and outer membrane to transfer electrons from their cellular metabolism to external electron acceptors[4,5,6,7,8]. Electroactive microbes can colonize electrode surfaces and form conductive biofilms, enabling long-distance electron transport across neighboring cells on the micrometer scale[9,10]. Electrochemical techniques are widely used to investigate electron transport mechanisms in these biofilms, demonstrating that redox gradient-driven electron hopping underlies biofilm conduction in both *G. sulfurreducens* and *S. oneidensis*[11,12,13]. These electroactive biofilms can serve as living biomaterials and form the basis of living electronics—hybrid systems that integrate cells with electrodes to combine the dynamic functionality of living cells with the input–output properties of electronic components[9,14,15].

A key challenge in developing such living electronic systems is the precise control of biofilm formation with respect to solid-state electrodes. Native biofilm formation often results in films that are non-uniform or too thin for reproducible electronic applications[12].

Copyright © 2026, Journal of Visualized Experiments

DOI 10.3791/74185

Although some electroactive bacteria, such as *G. sulfurreducens*, can form thicker biofilms[13], the lack of precise control over biofilm formation remains a major limitation for advancing these technologies. Therefore, to realize such hybrid systems, it is essential to develop new tools that enable high-resolution spatial control of electroactive biofilm formation on solid-state electrodes.

Inspired by photolithographic techniques used in solid-state electronics, previous work by the authors demonstrated the use of light to control the formation of conductive biofilms on electrodes[16]. By coupling light-responsive domains with transcription factors, optogenetic tools allow for precise spatial control of gene expression in bacteria[17,18,19]. This capability allows a wide range of bacterial activities to be tuned with high spatiotemporal precision[20,21,22,23]. Recently, bacterial biofilm patterning has been achieved using light-induced genetic circuits that control the expression of aggregation proteins mediating cell–cell adhesion[21,22]. For example, the blue light-inducible pDawn system has been used to regulate the expression of the cell-surface adhesin Ag43 to pattern *Escherichia coli* biofilms[21]. Inspired by these robust optogenetic patterning approaches, previous work by the authors implemented a similar strategy in the model EET organism *S. oneidensis* MR-1, enabling light-induced patterning of electroactive biofilms by using the blue light-responsive pDawn circuit to control the expression of the aggregation proteins CdrAB[16].

Here, a comprehensive protocol for patterning conductive biofilms on electrodes, measuring biofilm conduction, and calculating the intrinsic conductivity of these living materials was presented. This protocol first describes the construction of bioreactors with transparent electrodes serving as the base (**Figure 1**). Two approaches for biofilm patterning on these transparent electrodes are then presented (**Figure 1**). Following patterning, electrochemical measurements are performed to measure the conduction currents through the patterned biofilms (**Figure 1**), demonstrating that biofilm conduction depends on deposited pattern size. Using the measured conduction currents, the defined geometry of patterned biofilms, and biofilm thickness obtained from confocal microscopy, the intrinsic conductivity of these living conductive materials can be calculated (**Figure 1**). This technique offers a promising platform to enable further innovations in both the study and application of bioelectronics.

Protocol

The reagents and the equipment used are listed in the **Table of Materials.**

1. Bioreactor construction

NOTE: Transparent-bottom bioreactors are utilized to culture *S. oneidensis* cells for biofilm patterning onto the surface of transparent working electrodes (WEs) in advance of electrochemical measurements of patterned biofilms. Planar 22 mm by 40 mm commercial indium tin oxide (ITO) coated glass coverslips (see **Table of Materials**) or custom ITO interdigitated array (IDA) electrodes (see **Table of Materials** for fabrication information) are used as the transparent WEs and bases of the bioreactors.

1. Sequentially rinse the commercial ITO-coated glass coverslips and the custom ITO IDAs with acetone, isopropanol, and DI water from separate wash bottles, collecting the waste solvents in an appropriate waste container. Then dry the electrodes with N_2.

2. Adhere glass tubes (25 mm tall with a 19 mm and 22 mm inner and outer diameter, respectively) to the middle of the ITO-coated glass coverslips or over the interdigitated area of the ITO IDAs with siliconized sealant and leave the sealant to dry overnight.

   NOTE: As the sealant dries overnight, ensure the glass tube is uncovered so there is proper airflow to dry the sealant on the inside of the vessel.

3. Electrically connect thin copper wires to the ITO-coated glass coverslips and the custom ITO IDAs with silver paint. Strengthen the wire-electrode connections by covering them with epoxy. Leave the silver paint and the epoxy to dry overnight.

   NOTE: For the planar ITO-coated glass coverslips, attach a single wire near the edge of the electrode. For the ITO IDAs, attach one wire to each of the two contact pads corresponding to the two electrode arrays.

4. Check the bioreactors for leaks by filling the glass tubes with water and allowing them to sit for several hours.

5. Place the bioreactors in a covered container for autoclaving. In a separate covered container, place the custom three-port PEEK plastic lids with their custom Pt wire counter electrodes (CEs) for autoclaving (see **Table of Materials** for fabrication information).

   NOTE: Recycled P1000 micropipette tip racks work well to contain the bioreactors and lids for autoclaving. Custom three-port PEEK plastic lids, along with custom Pt wire CEs and commercial 1 M KCl Ag/AgCl reference electrodes (REs) (see **Table of Materials**), are used with the bioreactors. Autoclave the lids only with the custom Pt wire CEs. Do not autoclave the REs. The REs can be sterilized by wiping with 70% ethanol three times, allowing approximately

Copyright © 2026, Journal of Visualized Experiments

DOI 10.3791/74185

1 min of contact time, followed by wiping three times with sterile DI water. The CEs and REs can be held in place of the PEEK lid ports with Teflon tape. Perform blank electrochemical measurements on sterile bioreactors before biofilm patterning to confirm that the electrochemical setup is functioning properly. Detailed procedures for the electrochemical measurements are provided in Sections 4 and 5.

2. Preparation of the CdrAB strain for biofilm patterning

NOTE: An engineered *S. oneidensis* strain carrying the light-inducible plasmid pDawn-CdrAB was used for biofilm patterning[16]. The strain was constructed by transforming *S. oneidensis* MR-1 with pDawn-CdrAB. The plasmid contains a blue-light-inducible promoter that controls the expression of the aggregation proteins CdrAB, which promote cell–cell aggregation and enhance biofilm formation. Hereafter, this engineered *S. oneidensis* strain is referred to as the CdrAB strain.

1. Inoculate 5 mL of lysogeny broth (LB) medium (10 g/L tryptone, 5 g/L yeast extract, and 5 g/L sodium chloride) supplemented with 100 µg/mL streptomycin or spectinomycin for plasmid maintenance with a frozen stock of the CdrAB strain in a 14 mL culture tube. Cover the tube with aluminum foil and incubate overnight at 30 °C with shaking at 0.56 g.

   NOTE: Always cover the entire culture tubes with aluminum foil to prevent unwanted light exposure and avoid premature CdrAB expression in the preliminary cultures.

2. Subculture 50 µL of the saturated overnight culture of the CdrAB strain into 5 mL of fresh LB medium supplemented with 100 µg/mL streptomycin or spectinomycin in a 14 mL culture tube. Incubate the culture until it reaches the late logarithmic phase (OD_{600nm} ≈ 1.0–1.5, typically takes 6–8 h) at 30 °C with shaking at 0.56 g.

3. Dilute the late-log-phase CdrAB culture into fresh *S. oneidensis* M1 minimal medium supplemented with 100 µg/mL streptomycin or spectinomycin to an OD_{600nm} of 0.01. Add 1 or 2 mL of the diluted culture to the glass tube of each bioreactor, depending on the biofilm patterning approach used in the following section. Seal each glass tube with a 0.2 µm gas-permeable flask seal.

   NOTE: *S. oneidensis* M1 minimal medium contains 15.1 g/L PIPES buffer, 3.4 g/L sodium hydroxide, 1.5 g/L ammonium chloride, 0.1 g/L potassium chloride, 0.6 g/L sodium phosphate monobasic monohydrate, 3.36 g/L 60% (w/w) sodium lactate, 1 mL/L mineral solution, 1 mL/L vitamin solution, and 10 mL/L amino acid solution (pH 7.0)[16]. The composition details for the mineral, vitamin, and amino acid solutions are provided in **Supplementary Table 1**. The addition of 40 mM sodium fumarate is recommended to support cell growth and improve the sharpness of the biofilm pattern, but it is not required for successful biofilm patterning. At this stage, the bioreactors are used solely as culture vessels for the CdrAB cells. The PEEK plastic lids, Pt wire CEs, and REs are not used until the electrochemical measurements. The LB preculture with an OD_{600nm} of 1.0–1.5, the initial OD_{600nm} of 0.01 in the minimal medium, and the culture volume in the glass tube (1 or 2 mL, depending on the biofilm patterning approach used) were optimized to achieve reproducible and robust biofilm patterning.

3. Blue-light-induced biofilm patterning under aerobic conditions

NOTE: In this protocol, rectangular blue-light patterns (for example, a 1.3 × 1 cm^2 rectangle) are used. The bioreactors containing the cell cultures (1 mL for projector-based patterning and 2 mL for LED-based patterning) are used for biofilm patterning by either of the two approaches described below.

1. Pattern biofilms by two different approaches
   1. Pattern biofilms *via* projector (**Figure 2A**)
      1. Place the bioreactor inside a cardboard box mounted to the ceiling of the static incubator. The cardboard box is used to secure the bioreactor above the projector. Ensure that the bottom of the cardboard box contains an opening directly beneath the bioreactor to allow the projected blue light to pass through.
      2. Connect the portable smart projector (see **Table of Materials**) to the power supply and position it beneath the cardboard box. Project blue-light patterns (440 nm), created in Microsoft PowerPoint, onto the center of the bottom surface of the bioreactor. Place an adjustable neutral density filter at the projector aperture if necessary and adjust the blue-light intensity at the bottom surface of the bioreactor to 110 µW/cm^2, as measured using an optical power meter.

         NOTE: The uniformity of the projector illumination can be evaluated by projecting a larger illuminated area and measuring the light intensity at multiple locations.

Copyright © 2026, Journal of Visualized Experiments

DOI 10.3791/74185

3. Adjust the projector focus to obtain a sharp projection of the blue-light pattern on the electrode surface. Adjust the positions of both the projector inside the incubator and the bioreactor within the cardboard box to ensure that the projected blue-light pattern is centered at the desired location on the electrode surface. Perform biofilm patterning at 30 °C for 16 h with no agitation.

   NOTE: Before placing the setup in the incubator, project the blue-light pattern onto a wall positioned at the same distance from the projector as the bioreactor bottom will be inside the incubator. Adjust the pattern dimensions in Microsoft PowerPoint so that the projected blue-light pattern has the desired dimensions when projected onto the bottom surface of the bioreactor. This projector-based biofilm patterning setup offers several advantages: (1) it is inexpensive; (2) it is compatible with a variety of culture vessels, provided they can be securely positioned above the projector; (3) blue-light patterns can be easily designed and modified using Microsoft PowerPoint.

2. Pattern biofilms with a light-emitting diode (LED) array and photomask (**Figure 2B**)

   1. Place the blue-light LED board (468 nm; see **Table of Materials**) on the shelf of the incubator and connect it to the power supply. Connect the LED board to a computer and adjust the blue-light intensity to 110 μW/cm^{2,} as measured using an optical power meter.

   2. Prepare a photomask with the same dimensions as the LED board by creating an inverted (negative) image of the desired pattern. Print the photomask onto a transparency sheet using a laser printer so that the desired pattern remains transparent while the surrounding area is printed in black. Reprint the transparency approximately five times to achieve sufficient opacity for blocking blue light, and then cut out the printed photomask.

   3. Place the light diffuser beneath the photomask and then place both on top of the LED board. Position the bioreactor on top so that the light diffuser and photomask are located between the LED light source and the bioreactor.

   4. Adjust the position of the bioreactor to ensure that the blue-light pattern is centered at the desired location on the electrode surface. Perform biofilm patterning at 30 °C for 21 h.

      NOTE: The patterning times were empirically optimized for each illumination setup; 16 h was used for the projector-based setup, whereas 21 h provided improved biofilm formation with the LED board-based setup. This LED board-based biofilm patterning setup offers several advantages: (1) it is well suited for biofilm patterning using the bioreactors described in this protocol; (2) it is simple to assemble and operate, requiring minimal alignment; and (3) it provides stable and reproducible illumination.

2. After biofilm patterning with either method 3.1.1 or 3.1.2, discard the minimal medium from the bioreactors and wash the biofilms three times with 1 mL of sterile PBS by agitating the bioreactors with an orbital shaker at 0.038 g for 1 min per wash. After the final wash, add 1 mL of sterile *S. oneidensis* minimal medium to each bioreactor.

3. Transfer the bioreactors to an anaerobic chamber for electrochemical measurements.

4. Cyclic voltammetry (CV) measurements of the patterned biofilms on ITO-coated glass coverslips

NOTE: CV measurements are performed using a four-channel potentiostat (see **Table of Materials**), allowing simultaneous measurements of up to four bioreactors. Alternatively, any research-grade multichannel potentiostat can be used.

1. Replace the medium in the reactors with 3 mL of anaerobic minimal medium containing lactate but without vitamins or fumarate for turnover CV measurements.

2. Place the PEEK plastic lids, together with the custom Pt wire counter electrodes (CEs) and 1 M KCl Ag/AgCl reference electrodes (REs), onto the bioreactors.

3. Connect the black and white wires with red clips together and connect them to the working electrode (WE). Connect the black and white wires with black clips together and connect them to the CE. Connect the green wire with the black clip to the RE.

   NOTE: This step is based on the Squidstat potentiostat connection cables. If using an alternative potentiostat, connect the WE, CE, and REs to the appropriate cables on the potentiostat.

4. Perform CV scans from −500 mV to 300 mV versus the RE at a scan rate of 1 mV/s in the positive scan direction.

Copyright © 2026, Journal of Visualized Experiments

DOI 10.3791/74185

NOTE: Perform three CV cycles and analyze only the third cycle. This ensures that the analyzed results being looked at are free from any transient redox reactions or startup non-Faradaic effects arising from initiating the potential scan.

5. Electrochemical gating measurements of patterned biofilms on ITO IDAs

NOTE: The interdigitated region of each ITO IDA consists of 200 pairs of electrode fingers, each 12 mm long and 10 µm wide, separated by 15 µm gaps. Each device has a total working electrode area of 0.48 cm^2 (Design files are available on Zenodo: https://doi.org/10.5281/zenodo.21652394). IDA electrodes contain a set of two working electrodes, referred to as the source and drain electrodes. Electrochemical gating measurements are performed by simultaneously scanning both working electrodes while maintaining a fixed potential offset (V_{SD}), which drives electron transport laterally through the biofilm, bridging the source and drain electrodes. In this protocol, electrochemical gating measurements were performed using a bipotentiostat configuration with either two synchronized, single-channel potentiostats or a multichannel potentiostat (see **Table of Materials**). Alternatively, any research-grade bipotentiostat configuration that allows simultaneous and coordinated control of two working electrodes can be used.

1. Replace the medium in each reactor with 3 mL of anaerobic minimal medium without lactate, vitamins, or fumarate for non-turnover electrochemical gating measurements.
2. Place the PEEK plastic lids, together with the custom Pt wire CEs and 1 M KCl Ag/AgCl REs, onto the bioreactors.
3. Perform electrochemical gating measurements using one of the following potentiostat configurations.

   NOTE: The following cable connections and software setup are specific to the two synchronized, single-channel potentiostats and the multichannel potentiostat used by the authors. If using an alternative bipotentiostat configuration, connect the WEs, CE, and RE according to the instrument configuration and use the corresponding software settings for electrochemical gating measurements.

   1. Use two single-channel potentiostats.
      1. Connect the two single-channel potentiostats using a synchronization cable.
      2. Connect the red and orange clips from each potentiostat together to form one CE connection. Join the CE connections from the two potentiostats, and then connect the combined connection to the CE. Connect the white clips from the two potentiostats together, and then connect the combined connection to the RE. Connect the green and blue clips from each potentiostat together to form one WE connection for each potentiostat. Then, connect the resulting two WE connections to the two WEs.
      3. In the software of the potentiostat, select Linked Gating Cyclic Voltammetry and perform CV scans from −500 mV to 300 mV at a scan rate of 1 mV/s while maintaining a fixed gating offset of V_{SD} = 20 mV, where $V_{SD} = E_D - E_S$ and E_D and E_S are the potentials applied to the drain and source working electrodes, respectively.
   2. Use a multichannel potentiostat.
      1. In the software of the potentiostat, synchronize a pair of channels by selecting the first channel and then holding Ctrl while selecting the second channel.

         NOTE: Ensure that the 'Electrode Connections' setting is set to 'CE to ground'.
      2. Click on **Experiment** and then **Load Settings**. Load the Source.mps file onto the first channel and the Drain.mps file onto the second channel.
      3. Set the source channel to perform a CV scan from −500 mV to 300 mV at a scan rate of 1 mV/s. Set the drain channel to perform a CV scan from −480 mV to 320 mV at the same scan rate.

         NOTE: This configuration maintains a constant gating offset of V_{SD} = 20 mV.
      4. Connect the black and light blue wires from each channel together to form one CE connection. Join the CE connections from the two channels, and then connect the combined connection to the CE. Connect the white wires from the two channels together, and then connect the combined connection to the RE. Connect the red and pink wires from each channel together to form one WE connection per channel. Connect the resulting two WE connections to the two WEs. Run the experiment.

         NOTE: The conduction current of patterned biofilms bridging the source and drain WEs was measured as the potentials were swept at each WE. Perform three CV cycles and analyze only the third cycle.

Copyright © 2026, Journal of Visualized Experiments

DOI 10.3791/74185

6. *In situ* confocal microscopy, biofilm thickness analysis, and crystal violet staining of patterned biofilms

NOTE: Confocal microscopy, including FM 4-64FX staining and glutaraldehyde fixation of patterned biofilms, is typically performed after completion of the electrochemical measurements, and crystal violet staining is typically performed after confocal microscopy.

1. Discard the medium from the reactors and add 2 mL of *S. oneidensis* minimal medium containing 0.25 µg/mL FM 4-64FX membrane dye to fluorescently label biofilm cells. Incubate the biofilms in the dark for 30 min to allow membrane staining.
2. Replace the staining solution with 2 mL of 3% glutaraldehyde and fix the cells overnight at 4 °C.
3. Rinse the samples three times with 2 mL of PBS. Leave the PBS from the final rinse in the bioreactors for imaging.
4. Image multiple regions within the patterned biofilms on the electrodes using an inverted confocal microscope equipped with an argon laser and a 20× dry objective.
5. Analyze the confocal image stacks using Imaris software to generate three-dimensional reconstructions and cross-sectional images of the biofilms.
6. Determine the biofilm thickness by analyzing the cross-sectional confocal images using MATLAB.

   NOTE: Biofilm thickness can be determined from confocal microscopy images using a variety of image analysis methods. In this work, biofilm thickness was analyzed using the same method described in a previous publication by the authors[16]. The detailed procedure and MATLAB code are provided in **Supplementary File 1**.
7. Stain the patterned biofilms with 1 mL of 0.1% crystal violet for 10 min, rinse three times with 2 mL of PBS, and dry at room temperature to visualize the biofilm patterns.

   NOTE: Crystal violet is retained by biofilms and is commonly used to confirm the presence of bacterial biofilms and quantify biofilm formation. The purpose of crystal violet staining in this protocol is to provide a quick check that biofilm patterning occurred as expected after electrochemical measurements and confocal microscopy.

7. Quantification of the intrinsic conductivity of living biofilms from electrochemical gating measurements and defined biofilm geometry

1. Determine the conduction current (I_{cond}) through the patterned biofilms bridging the source and drain electrodes by subtracting the drain and source currents and dividing by two, $I_{cond} = (I_D - I_S) / 2$, where I_D is the drain current and I_S is the source current. Plot the I_{cond} as a function of the gate potential (E_G), defined as the average potential of drain and source WEs during the gating scan, to determine the peak conduction current.

   NOTE: This calculation assumes that the drain and source WEs measure conduction currents of equal magnitude but opposite sign, together with background currents of the same sign.
2. Calculate the conductivity of the patterned biofilms based on the following equations[12,13,24,25].

   $I_{cond} = G \cdot V_{SD}$ (1)

   $G = \sigma \cdot S$ (2)

   $$S = \frac{l}{\pi} ln\left(\frac{8g}{\pi a}\right) \quad (3)$$

   (Use this equation when the biofilm thickness is on the order of the finger gap, as in this protocol)

   $$S = \frac{l}{\pi} ln\left(\frac{4b}{a}\right) \quad (4)$$

   (Use this equation when the biofilm thickness is much larger than the finger gap)

   NOTE: Equation 1 is used to determine biofilm conductance (G). Here, I_{cond} is given by the peak conduction current and V_{SD} = 20 mV. In Equation 2, G is equal to the intrinsic conductivity of the biofilm (σ) multiplied by a geometric factor (S) dependent on the electrode and biofilm geometries. For the case of a uniform biofilm on an IDA with a thickness on the order of the width of the finger gap, the geometric factor S is shown as Equation 3, based on a conformal mapping method[25]. For the case where a uniform biofilm on an IDA possesses a thickness much larger than the width of the finger gap, the geometric factor S is shown as Equation 4. In Equations 3 and 4, l is the length of the gap that snakes between the interdigitated fingers and can be calculated by multiplying the number of patterned biofilm-covered gaps by the length of each gap, g is the biofilm thickness, a is half the width of the finger gap, and b is the electrode finger width plus a. Additionally, Equation 1 assumes a linear relationship between I_{cond} and V_{SD}. To verify this assumption, measure I_{cond} over a range of V_{SD} values and confirm that a plot of I_{cond} versus V_{SD} is linear. Previous studies by the authors have

Copyright © 2026, Journal of Visualized Experiments

DOI 10.3791/74185

demonstrated this linear relationship over a V_{SD} range of 10–70 mV[16,26].

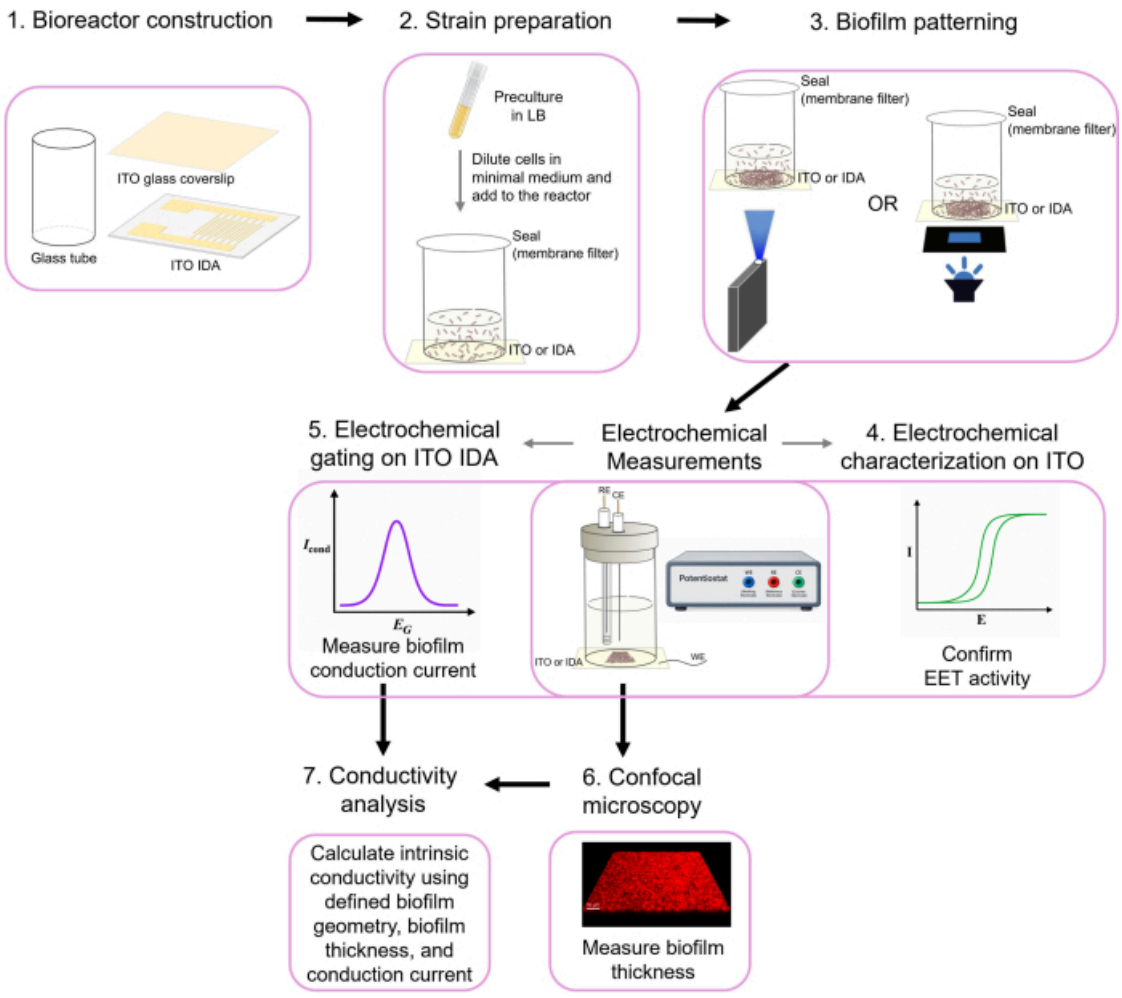


Figure 1: Overall schematic of the experimental workflow described in this protocol. Please click here to view a larger version of this figure.

Results

Biofilm patterning can be performed using either a projector-based or an LED board-based setup (**Figure 2A**,**B**). In this protocol, *S. oneidensis* biofilms were patterned into rectangular geometries on two types of transparent electrodes, ITO-coated glass coverslips and custom ITO interdigitated array (IDA) electrodes, using either projected rectangular blue-light patterns designed in Microsoft PowerPoint or blue light from an LED board projected through printed rectangular photomasks. Crystal violet staining revealed a well-defined rectangular biofilm pattern of the CdrAB strain on the electrode surface following cultivation in the bioreactors under blue-light illumination (**Figure 2C**). The line edge roughness of the rectangular biofilm pattern on the ITO IDA using the projector-based setup was previously quantified as 37.5 µm and 51.3 µm for the left and right edges, respectively[16]. Line edge roughness was determined from fluorescence micrographs as the root-mean-square deviation of each identified biofilm edge from a linear regression, as described previously[16]. In addition, individual biofilm strips with a width of approximately 650 µm were successfully patterned using this system[16]. Thus, this patterning approach provides sufficient spatial control over conductive biofilm geometry.

After biofilm patterning, cyclic voltammetry (CV) measurements were performed on biofilms patterned on the ITO-coated glass coverslips (**Figure 2D**). Experiments were performed using three independent replicate bioreactors for each patterned biofilm condition and the dark control condition. Representative

Copyright © 2026, Journal of Visualized Experiments

DOI 10.3791/74185

measurements from individual bioreactors are shown. The results showed that the patterned *S. oneidensis* biofilms of the CdrAB strain retained their ability to reduce electrodes, exhibiting a characteristic redox response corresponding to outer membrane cytochromes (**Figure 2E**). Under the experimental conditions described above, the light-patterned biofilms of the CdrAB strain generated higher currents than non-patterned biofilms formed by the CdrAB strain cultured under dark conditions (**Figure 2E**). This is due to enhanced biofilm formation on electrodes after expressing the CdrAB proteins[16].

Next, electrochemical gating measurements on biofilms patterned on ITO IDA electrodes were performed to investigate long-distance electron transport through *S. oneidensis* biofilms and quantify their conductivity (**Figure 3A**). Three biofilm patterns with different dimensions were generated on ITO IDA electrodes: 1.3 × 0.25 cm^2 (small), 1.3 × 0.5 cm^2 (medium), and 1.3 × 1 cm^2 (large, covering the entire IDA area). Electrochemical gating was then used to measure the conduction current (I_{cond}) through the patterned biofilms bridging the source and drain electrodes. Experiments were performed using two independent replicate bioreactors for each pattern size. Representative measurements from individual bioreactors are shown. Plotting the conduction current (I_{cond}) as a function of gate potential (E_G) revealed peak-shaped curves centered at the redox potential of *S. oneidensis* EET proteins (**Figure 3B**), as expected for a redox conduction mechanism, demonstrating cell-to-cell long-distance electron transport within the light-patterned biofilms[13]. Furthermore, the conduction current increased with increasing biofilm size (**Figure 3B**), consistent with the larger biofilms providing a greater conductive channel between the source and drain electrodes. Crystal violet staining further confirmed the successful formation of the three biofilm patterns with the expected dimensions (**Figure 3B**). These results demonstrate that biofilm conduction can be precisely controlled by defining the geometry of the patterned biofilms, an important capability for developing more advanced living electronics.

Confocal microscopy showed that the patterned biofilms are thick and uniform with a representative thickness of approximately 10 µm (**Figure 3C** and **Supplementary File 1**). By using the defined biofilm geometry produced through light patterning, biofilm thickness measured by confocal microscopy, and conduction current measured *via* electrochemical gating, the intrinsic conductivity of living *S. oneidensis* biofilms could be determined. Since the patterned biofilm thicknesses were on the order of the ITO IDA electrode finger gap, Equations 1–3 were used to determine the *S. oneidensis* biofilm conductivity. For calculating the geometric factor *S* using Equation 3, *l* was determined from the number of patterned biofilm-covered gaps and the length of each gap, as described above. The 1.3 × 1 cm^2 pattern covered the entire IDA region, corresponding to 399 gaps, each 1.2 cm long; therefore, *l* was calculated as 399 × 1.2 cm. Since the 1.3 × 0.5 cm^2 and 1.3 × 0.25 cm^2 patterns covered one-half and one-quarter of the area of the 1.3 × 1 cm^2 pattern, respectively, their *l* values were calculated as 0.5 and 0.25 times the *l* value of the 1.3 × 1 cm^2 pattern. The parameter *a* was set to 7.5 µm, corresponding to half of the 15 µm finger gap, and *g* was set to 10 µm based on the representative biofilm thickness measured by confocal microscopy. The conductivity values calculated for each of the three biofilm pattern sizes were independent of pattern size, as expected, because conductivity is an intrinsic material property that describes its ability to conduct electricity. The measurements yielded an average conductivity of approximately 4.5 nS/cm across the three pattern sizes. This experimentally determined conductivity agrees well with the simulated conductivity (~7 nS/cm) predicted by a collision-exchange electron transport model that accounts for the dynamics of outer-membrane cytochromes[27].

Copyright © 2026, Journal of Visualized Experiments

DOI 10.3791/74185

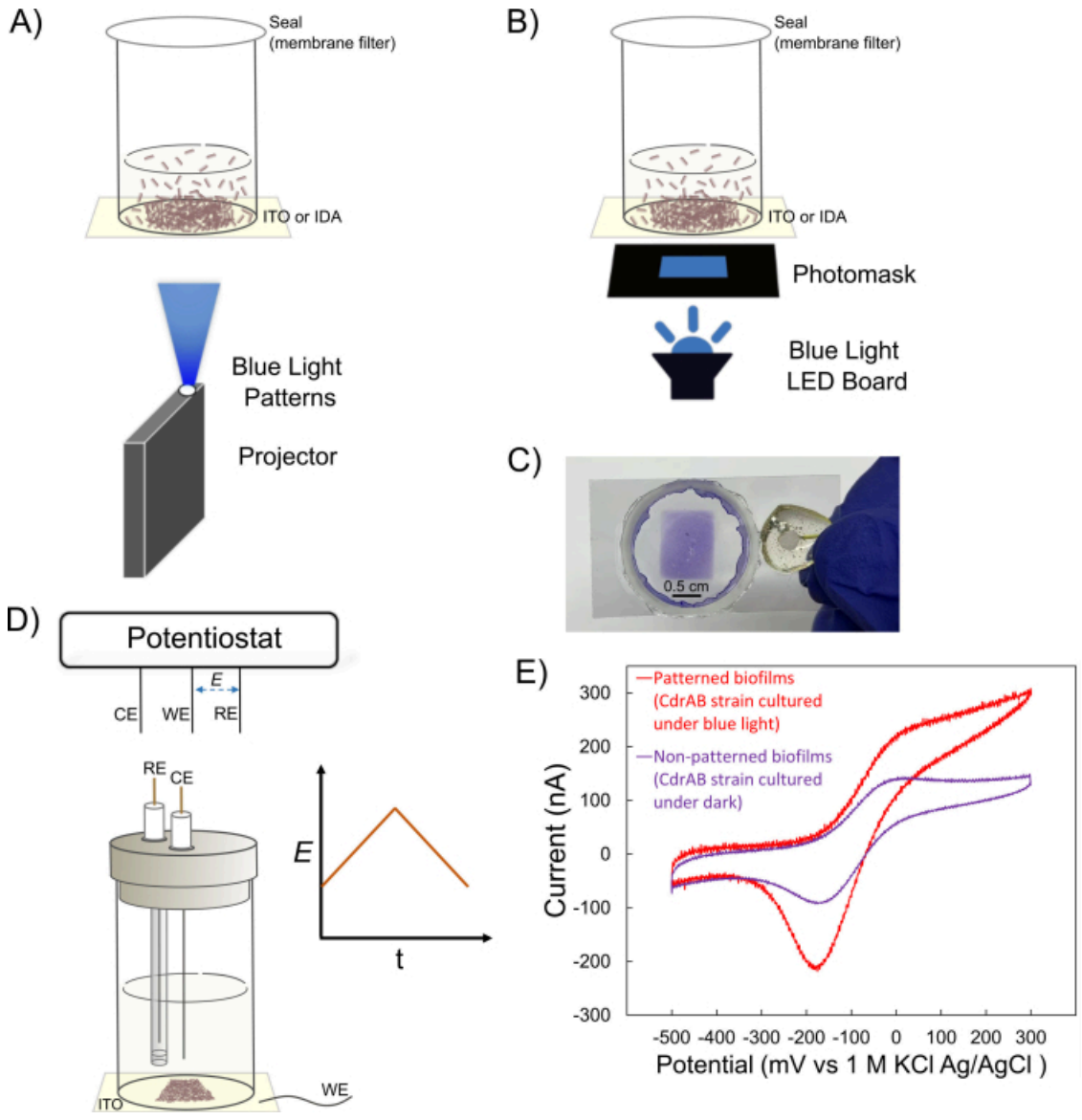


Figure 2: Biofilm patterning of the CdrAB strain on transparent electrodes and electrochemical characterization of the patterned biofilms. (**A**) Schematic diagram of the projector-based biofilm patterning setup. (**B**) Schematic diagram of the LED board-based biofilm patterning setup. (**C**) Crystal violet staining of a patterned CdrAB biofilm on an ITO-coated glass coverslip using the projector-based biofilm patterning setup. Scale bar: 5 mm. (**D**) Schematic diagram of the bioreactor and three-electrode configuration used for electrochemical measurements on ITO, including the working electrode (WE), reference electrode (RE), and counter electrode (CE). (**E**) Representative cyclic voltammograms of light-patterned CdrAB biofilms and non-patterned CdrAB biofilms cultured under dark conditions on ITO-coated glass coverslips from representative bioreactors. Panels (**A**) and (**E**) were adapted from Zhao et al.[16]. Please click here to view a larger version of this figure.

Copyright © 2026, Journal of Visualized Experiments

DOI 10.3791/74185

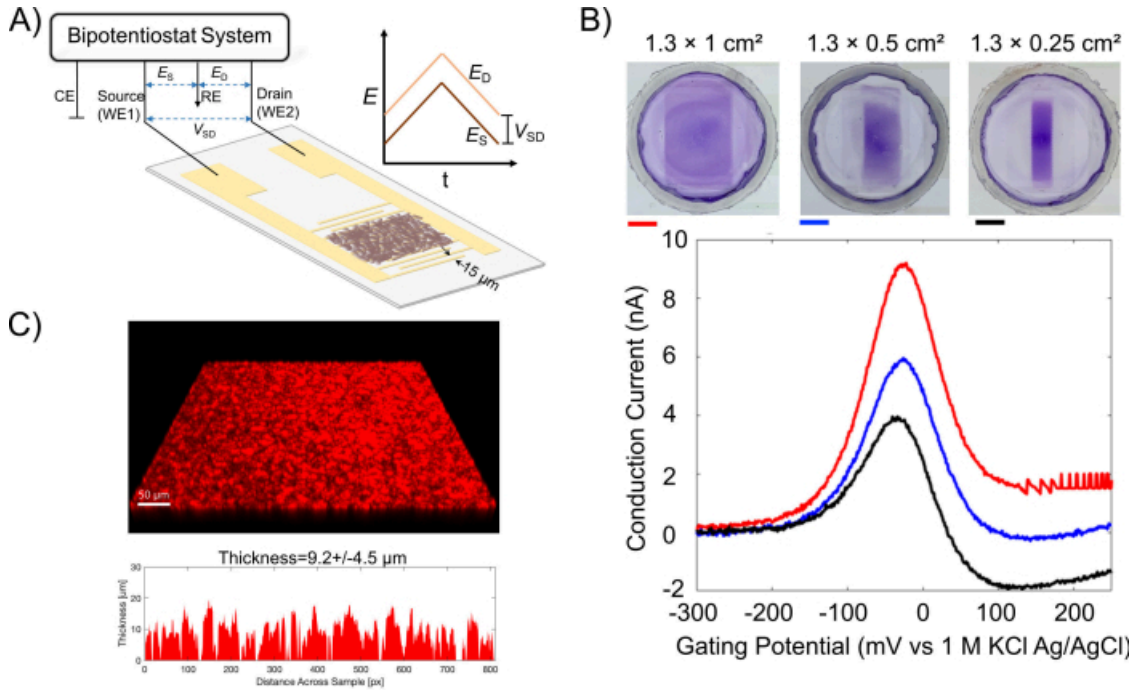


Figure 3: Electrochemical gating measurements of conduction current (I_{cond}) and biofilm conductivity. (**A**) Schematic diagram of the custom transparent ITO IDA electrode and bipotentiostat configuration used for electrochemical gating measurements, showing the source and drain working electrodes (WE1 and WE2) and the source-drain potential offset (V_{SD}). (**B**) Crystal violet staining of representative patterned biofilms with different pattern sizes after electrochemical measurements and representative conduction current curves for the corresponding biofilm patterns from individual bioreactors (biofilms were patterned using the projector-based setup). (**C**) Representative three-dimensional confocal microscopy image of a region within the 1.3 × 1 cm² patterned biofilms and representative biofilm thickness measurement obtained from a cross-sectional confocal image using MATLAB[16]. Panel (**B**) was adapted from Zhao et al.[16]. Please click here to view a larger version of this figure.

Supplementary Table 1: The composition details for the mineral, vitamin, and amino acid solutions of *S. oneidensis* M1 minimal medium. Please click here to download this file.

Supplementary File 1: Method for biofilm thickness analysis using MATLAB. Please click here to download this file.

Discussion

This protocol provides a biofilm lithography approach for controlled measurements of the model electroactive bacterium *S. oneidensis* on electrode surfaces using an engineered *S. oneidensis* strain containing a blue-light-inducible genetic circuit that controls the expression of the cell aggregation proteins CdrAB. Although this protocol was developed for *S. oneidensis*, the overall strategy could potentially be adapted to other electroactive bacteria. It remains unclear whether the pDawn-CdrAB system can function effectively in other electroactive bacteria; however, biofilm patterning may be achieved by coupling light-inducible genetic circuits to other aggregation systems, such as Ag43[21] or SpyTag/SpyCatcher[28]. Alternatively, native aggregation and biofilm-forming systems in the target electroactive organism could potentially be engineered for light-inducible control. The protocol integrates a wide range of techniques, including bioreactor construction, bacterial cell culturing, optogenetic operation, electrochemical measurements and analysis, *in situ* confocal microscopy, and mathematical modeling for biofilm conductivity calculations.

To ensure proper bioreactor assembly, it is recommended to check the bioreactors for leaks before biofilm patterning. In addition, blank electrochemical measurements should be performed before using the bioreactors as biofilm patterning culture vessels to confirm that the electrochemical setup is functioning properly.

Several factors should be considered during biofilm patterning. First, dilution of the CdrAB strain from an LB preculture into *S. oneidensis* minimal medium is a critical step. An LB preculture with an OD_{600nm} of 1.0–1.5 and an initial OD_{600nm} of 0.01 in the minimal medium is recommended. Successful biofilm patterning requires appropriate cell growth and cell density in the bioreactor. Diluting an LB preculture at an OD_{600nm} of 1.0–1.5 into minimal medium with an initial OD_{600nm} of 0.01 provides both an appropriate starting cell density and a small amount of residual LB medium that

Copyright © 2026, Journal of Visualized Experiments

DOI 10.3791/74185

modestly supports initial cell growth without substantially altering the minimal medium composition. In contrast, washing cells from the LB preculture and resuspending them in minimal medium before dilution often results in poor cell growth and weak biofilm patterning. Conversely, culturing the CdrAB strain directly in LB medium during patterning promotes rapid cell growth and biofilm formation at the air–liquid interface rather than on the electrode surface. Second, the patterning duration, culture volume in the bioreactor, and illumination intensity used in this protocol were optimized for the projector-based and LED board-based patterning setups described here. If different patterning setups or bioreactors are used, these parameters may need to be re-optimized. Third, supplementation of the minimal medium with fumarate supports the growth of the CdrAB strain and improves the sharpness of the patterned biofilms.

After biofilm patterning, washing the bioreactors while shaking them on an orbital shaker is an important step because it removes loosely attached cells from the unexposed regions of the electrode, thereby improving the spatial resolution of pattern-size-dependent conduction current measurements.

This method also has several limitations. First, it is not suitable for patterning biofilms on non-transparent electrodes because light must pass through the electrode substrate from below during illumination. Patterning on non-transparent but optically accessible electrodes may be possible with adaptations to the illumination setup. For example, increasing the light intensity, using a stronger light source, or extending the patterning duration may help compensate for light attenuation through the culture. Alternatively, illuminating the bioreactor from above and passing light through the culture could enable patterning on non-transparent electrodes. In this configuration, parameters such as patterning duration, culture volume, illumination intensity, and the initial cell density (OD_{600nm}) may need to be optimized to ensure that sufficient light reaches the electrode surface and that patterning occurs at the electrode rather than primarily near the culture surface. Second, although blue-light-induced expression of CdrAB promotes dense biofilm formation in illuminated regions of the electrode surface, some cells remain attached in unexposed regions and still produce measurable currents. Although orbital shaking during washing removes a portion of these cells, residual cells remain in the unexposed regions, limiting the spatial resolution of pattern size-dependent biofilm conduction measurements. Future work will focus on developing synthetic biology strategies to further eliminate cell attachment in non-patterned regions, such as introducing an additional light-inducible genetic circuit to express proteins that promote cell detachment or cell death[29].

In summary, a simple and versatile technique has been developed for directing the deposition of living conductive biofilms onto electrode surfaces. Sriram et al. subsequently applied this CdrAB strain and biofilm patterning approach for electrochemical impedance spectroscopy (EIS), using an equivalent circuit model with separate components representing electrode-biofilm interfacial resistance and biofilm charge-transfer resistance[30]. More recently, this technique was used by the authors to investigate the role of periplasmic cytochromes in outward EET and lateral biofilm conductivity in *S. oneidensis* by patterning periplasmic cytochrome-deficient mutant strains on electrode surfaces[31], and to develop living electronic transistors with tunable conductivity through cytochrome doping in patterned *S. oneidensis* biofilms[26]. This approach is expected to enable further innovations in both the study and application of microbial bioelectronics.

Disclosures

`The authors have no conflicts of interest to disclose.

Acknowledgments

This study was supported by the US Office of Naval Research Multidisciplinary University Research Initiative Grant No. N00014-18-1-2632. J.T.A. was supported by the NSF Postdoctoral Research Fellowships in Biology Program under grant no. 2010604. J.Q.B. acknowledges support from the Army Research Office under cooperative agreement number W911NF-24-2-0003.

References

1. Myers CR, Nealson KH. Bacterial manganese reduction and growth with manganese oxide as the sole electron acceptor. Science. 1988;240:1319-1321.
2. Lovley DR, Phillips EJP. Novel mode of microbial energy metabolism: organic carbon oxidation coupled to dissimilatory reduction of iron or manganese. Appl Environ Microbiol. 1988;54:1472-1480.
3. Gralnick JA, Bond DR. Electron transfer beyond the outer membrane: putting electrons to rest. Annu Rev Microbiol. 2023;77:517-539.
4. McMillan DG, Marritt SJ, Butt JN, Jeuken LJM. Menaquinone-7 is a specific cofactor in tetraheme quinol dehydrogenase CymA. J Biol Chem. 2012;287:14215-14225.
5. Dohnalkova AC, et al. Imaging hydrated microbial extracellular polymers: comparative analysis by electron microscopy. Appl Environ Microbiol. 2011;77:1254-1262.
6. Hartshorne RS, et al. Characterization of an electron conduit between bacteria and the extracellular environment. Proc Natl Acad Sci U S A. 2009;106:22169-22174.
7. White GF, et al. Rapid electron exchange between surface-exposed bacterial cytochromes and Fe(III) minerals. Proc Natl Acad Sci U S A. 2013;110:6346-6351.

Copyright © 2026, Journal of Visualized Experiments

8. Edwards MJ, et al. The crystal structure of a biological insulated transmembrane molecular wire. Cell. 2020;181:665-673.e10.
9. Zacharoff LA, El-Naggar MY. Redox conduction in biofilms: from respiration to living electronics. Curr Opin Electrochem. 2017;4:182-189.
10. Atkinson JT, Chavez MS, Niman CM, El-Naggar MY. Living electronics: a catalogue of engineered living electronic components. Microb Biotechnol. 2023;16:507-533.
11. Snider RM, Strycharz-Glaven SM, Tsoi SD, Erickson JS, Tender LM. Long-range electron transport in *Geobacter sulfurreducens* biofilms is redox gradient-driven. Proc Natl Acad Sci U S A. 2012;109:15467-15472.
12. Xu S, Barrozo A, Tender LM, Krylov AI, El-Naggar MY. Multiheme cytochrome mediated redox conduction through *Shewanella oneidensis* MR-1 cells. J Am Chem Soc. 2018;140:10085-10089.
13. Yates MD, et al. Thermally activated long-range electron transport in living biofilms. Phys Chem Chem Phys. 2015;17:32564-32570.
14. Zhang Y, Hsu LHH, Jiang X. Living electronics. Nano Res. 2020;13:1205-1213.
15. Yim SS, et al. Robust direct digital-to-biological data storage in living cells. Nat Chem Biol. 2021;17:246-253.
16. Zhao F, et al. Light-induced patterning of electroactive bacterial biofilms. ACS Synth Biol. 2022;11:2327-2338.
17. Levskaya A, et al. Engineering Escherichia coli to see light. Nature. 2005;438:441-442.
18. Ohlendorf R, Vidavski RR, Eldar A, Moffat K, Möglich A. From dusk till dawn: one-plasmid systems for light-regulated gene expression. J Mol Biol. 2012;416:534-542.
19. Tabor JJ, Levskaya A, Voigt CA. Multichromatic control of gene expression in Escherichia coli. J Mol Biol. 2011;405:315-324.
20. Zhao EM, et al. Optogenetic regulation of engineered cellular metabolism for microbial chemical production. Nature. 2018;555:683-687.
21. Jin X, Riedel-Kruse IH. Biofilm lithography enables high-resolution cell patterning *via* optogenetic adhesin expression. Proc Natl Acad Sci U S A. 2018;115:3698-3703.
22. Moser F, Tham E, González LM, Lu TK, Voigt CA. Light-controlled, high-resolution patterning of living engineered bacteria onto textiles, ceramics, and plastic. Adv Funct Mater. 2019;29:1-11.
23. Cheng X, et al. Engineering Gac/Rsm signaling cascade for optogenetic induction of the pathogenicity switch in Pseudomonas aeruginosa. ACS Synth Biol. 2021;10:1520-1530.
24. Blauch DN, Saveant JM. Dynamics of electron hopping in assemblies of redox centers. Percolation and diffusion. J Am Chem Soc. 1992;114:3323-3332.
25. Kankare J, Kupila EL. *In situ* conductance measurement during electropolymerization. J Electroanal Chem. 1992;322:167-181.
26. Atkinson JT. Living electronic transistors with tunable conductivity. bioRxiv. 2026. doi:10.64898/2026.09.01.748419.
27. Chong GW, et al. Single-molecule tracking of bacterial cell surface cytochromes reveals dynamics that impact long-distance electron transport. Proc Natl Acad Sci U S A. 2022;119:e2119964119.
28. Hartzell EJ, Terr J, Chen W. Engineering a blue light inducible SpyTag system (BLISS). J Am Chem Soc. 2021;143:8572-8577.
29. Zhao F, et al. Red-light-induced genetic system for control of extracellular electron transfer. ACS Synth Biol. 2024;13:1467-1476.
30. Sriram S, Olivan LA, White RJ, Rowe AR. Quantifying cathode biofilm resistance in a cdrAB modified *Shewanella oneidensis* MR-1 using electrochemical impedance spectroscopy. Electrochim Acta. 2024;481:143967.
31. Zhao F, et al. Light-directed biofilm formation reveals the functional contributions of periplasmic cytochromes to the electrochemical activity of *Shewanella oneidensis*. mBio. 2026. doi:10.1128/mbio.01264-26.

Copyright © 2026, Journal of Visualized Experiments